Inhibition of Podocyte FAK Protects against Proteinuria and Foot Process Effacement

Hong Ma,* Akashi Togawa,† Keita Soda,* Junhui Zhang,* Sik Lee,* Ming Ma,* Zhiheng Yu,* Thomas Ardito,‡ Jan Czyzyk,‡ Lonnette Diggs,* Dominique Joly,§ Shinji Hatakeyama,‖ Eiji Kawahara,‖ Lawrence Holzman,¶ Jun Lin Guan,** and Shuta Ishibe*

Departments of *Internal Medicine and ‡Pathology, Yale University School of Medicine, New Haven, Connecticut; †Department of Internal Medicine, Hamamatsu University School of Medicine, Hamamatsu, Japan; §Université Paris-Descartes, Faculté de Médecine, INSERM U813, Hôpital Necker-Enfants-Malades Paris, France; ‖Oncology Unit, Novartis Pharmaceuticals, Tokyo, Japan; and **Division of Molecular Medicine and Genetics, ¶Department of Internal Medicine, University of Michigan Medical School, Ann Arbor, Michigan

ABSTRACT

Focal adhesion kinase (FAK) is a nonreceptor tyrosine kinase that plays a critical role in cell motility. Movement and retraction of podocyte foot processes, which accompany podocyte injury, suggest focal adhesion disassembly. To understand better the mechanisms by which podocyte foot process effacement leads to proteinuria and kidney failure, we studied the function of FAK in podocytes. In murine models, glomerular injury led to activation of podocyte FAK, followed by proteinuria and foot process effacement. Both podocyte-specific deletion of FAK and pharmacologic inactivation of FAK abrogated the proteinuria and foot process effacement induced by glomerular injury. *In vitro*, podocytes isolated from conditional FAK knockout mice demonstrated reduced spreading and migration; pharmacologic inactivation of FAK had similar effects on wild-type podocytes. In conclusion, FAK activation regulates podocyte foot process effacement, suggesting that pharmacologic inhibition of this signaling cascade may have therapeutic potential in the setting of glomerular injury.

J Am Soc Nephrol 21: 1145–1156, 2010. doi: 10.1681/ASN.2009090991

The glomerulus forms the filtration barrier of the kidney and is composed of a fenestrated endothelium, glomerular basement membrane (GBM), and the podocytes that interdigitate to form slit diaphragms.[1,2] When the podocytes are damaged, foot process fusion occurs. This process involves the rearrangement of the actin cytoskeleton and retraction of the foot processes toward the cell body, allowing mechanical forces and signaling events to be transmitted into the cell. Since the identification that mutations of the podocyte slit diaphragm specific NPHS1 gene cause congenital nephrotic syndrome,[3–5] podocytes have been recognized as critical regulators of glomerular injury. Other podocyte slit diaphragm proteins such as podocin, synaptopodin, and CD2AP have generated further interest in the regulation of the kidney filtration barrier[6–8]; however, little is still known about cell–matrix interactions in podocytes. Mice lacking the focal adhesion protein integrin-linked kinase (ILK), specifically in the podocytes, also develop proteinuria, resulting in renal failure and death.[9] Moreover, mice lacking $\alpha 3\beta 1$ integrin have demonstrated inability to form mature foot processes.[10] These cell–matrix interactions, which seem important in podocyte development, may also play a critical role after podocyte injury, because the process of podocyte effacement

Received September 28, 2009. Accepted April 12, 2010.

Published online ahead of print. Publication date available at www.jasn.org.

Correspondence: Dr. Shuta Ishibe, 300 Cedar Street, TAC S369, New Haven, CT 06519. Phone: 203-785-4184; Fax: 203-785-4904; E-mail: shuta.ishibe@ yale.edu

requires cell process retraction and movement, processes that suggest focal adhesion disassembly.

Focal adhesion kinase (FAK) is a nonreceptor tyrosine kinase, in which integrin- or growth factor–induced autophosphorylation at tyrosine 397 results in activation of critical signaling pathways required for focal adhesion turnover.[11–16] It has been demonstrated that cell spreading and migration are significantly diminished in cells lacking FAK.[17] This inhibition in motility has brought excitement in cancer therapeutics, resulting in the development and use of FAK inhibitors.[18–21] In a recent study, inhibition of urokinase plasminogen activator (uPAR), a glycosylphosphatidylinositol-anchored protein that is important for cell invasion and metastasis, has been demonstrated to reduce proteinuria and podocyte effacement significantly, suggesting that this dynamic podocyte cell movement may mimic the molecular signaling events observed in cancer cell invasion.[22]

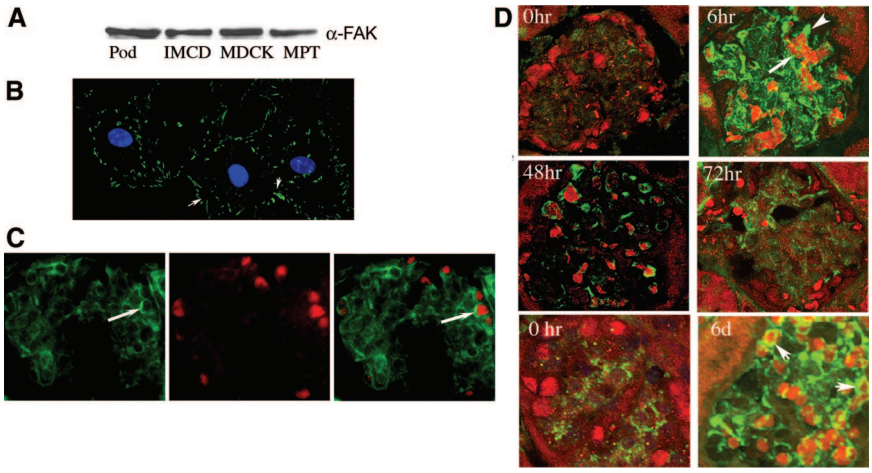

Figure 1. Podocyte injury activates FAK. (A) Whole-cell lysates from podocytes and IMCD, MCDK, and MPT cells immunoblotted with α-FAK. (B) Stable differentiated podocytes stained with α-FAK (green) to assess for focal adhesions. Arrow indicates focal adhesion complex. (C) Kidney cryosections stained with α-FAK (arrow, green), α-WT-1 (red), and merge. (D) Representative glomeruli from LPS-treated *FAK*$^{+/+}$*;Pod-Cre* mice at the indicated time points stained with α-pFAK Y397 (green; arrowhead at 6 hours) and with α-WT-1 (red; arrow at 6 hours). The bottom two panels represent representative glomeruli from *FAK*$^{+/+}$*;Pod-Cre* mice treated with rabbit anti-mouse GBM at day 6 stained with antibodies as above (arrows indicating pFAKY397).

In this study, we demonstrated that after podocyte injury *in vivo* and *in vitro*, FAK activation was significantly increased in wild-type (WT) mice, prompting us to address whether inhibition or loss of FAK activation would reduce podocyte cell motility by inhibiting focal adhesion turnover, thereby preventing proteinuria and effacement. Because complete FAK gene deletion results in lethality at embryonic day 8.5, a time point before glomerular development has been initiated, the ability to study this protein's role in podocyte development as well as repair after injury has been limited.[17] Hence, selective loss of FAK expression in the podocytes of the kidney was achieved using a Cre-loxP approach.[23,24] These mice were born without evidence of podocyte/glomerular developmental defects but were resistant to the foot process fusion and subsequent proteinuria that typically accompany LPS and rabbit anti-mouse GBM-induced podocyte damage. We postulate this inhibition of foot process effacement is due to diminished podocyte spreading and motility, supported by our *in vitro* data. In addition, pharmacologic treatment of WT mice using the FAK inhibitor TAE-226 significantly reduced proteinuria and podocyte effacement, raising the possibility for therapeutic use in glomerular diseases.

RESULTS

FAK is Expressed in Podocytes and Activated after Injury

FAK expression in podocytes was initially confirmed by Western blot (Figure 1A). To determine localization in podocytes, we performed immunofluorescence demonstrating FAK at sites of focal adhesions (Figure 1B). We next determined podocyte FAK expression *in vivo* by co-labeling with FAK and WT-1, a podocyte cell marker (Figure 1C). Even though total FAK expression was observed within the glomerulus by immunofluorescence in normal kidney sections (Figure 1C), the activated form of FAK (FAK Y397) was not observed (data not shown). Hence, to determine next whether FAK activation coincides with podocyte injury, we tested two animal models of podocyte injury resulting in proteinuria. Low-dosage LPS injection, a model of transient proteinuria,[25] resulted in robust FAK activation at Try 397, 6 hours after injection, which diminished after 72 hours (Figure 1D, top and middle). Because podocytes have been demonstrated to migrate into the Bowman's capsule during crescent formation,[26,27] we next tested the rabbit anti-mouse GBM model, which results in murine glomerulonephritis.[28] After induction, increased FAK activation within the glomerulus as well as podocytes was observed at 6 days (Figure 1D, bottom) and diminished by 12 days (data not shown).

Podocyte-Specific Deletion of FAK

To address further the importance of FAK activation within podocytes after *in vivo* murine models of podocyte injury, we generated a conditional podocyte knockout mouse model using the Cre-Lox system. *FAK*$^{fl/fl}$ mice, in which exon 3 of the *FAK* gene is flanked by loxP sites,[29,30] were mated with *Podocin-Cre* mice that express the Cre recombinase in the podocytes[24] (Figure 2A). Offspring that were heterozygous for the floxed FAK allele (*FAK*$^{fl/+}$*;Pod-Cre*) were mated to generate *FAK*$^{fl/fl}$*;Pod-Cre* and *FAK*$^{+/+}$*;Pod-Cre* offspring, confirmed by DNA genotyping of the tail (Figure 2B). *FAK*$^{fl/fl}$*;Pod-Cre* mice

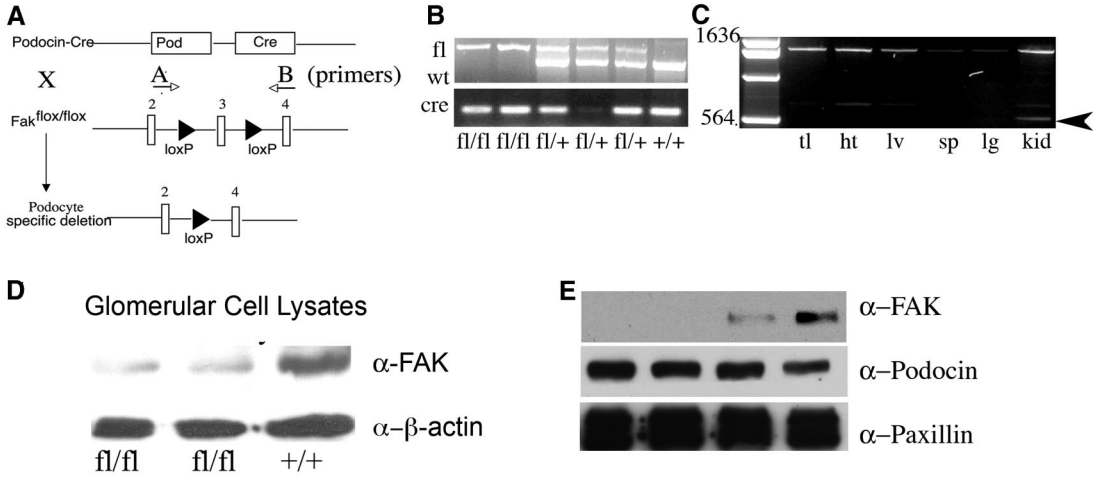

Figure 2. FAK is specifically deleted in podocytes. (A) Algorithm used to generate podocyte-specific FAK knockout mice (primer designated A and B). (B) Representative PCR analysis of extracted genomic DNA from mouse-tail clippings from $FAK^{fl/fl}$;*Pod*-Cre (1600 bp), $FAK^{+/+}$;*Pod*-Cre (1500 bp), and $FAK^{fl/+}$;*Pod*-Cre. (C) Representative PCR analysis of extracted genomic DNA assessing tissue specific excision of FAK. Controls from tail (tl), heart (ht), liver,[57] spleen (spl), and lung (lg) reveal an approximately 1.6-kb band that represents the nonexcised FAK gene product. The tissue-specific deletion of the loxP-flanked sequence of the podocytes of the renal cortex results in the expected 600-bp fragment (arrow) as well as a 1.6-kb product representing nonexcised genomic DNA, presumed mainly from the proximal tubule cells in this region (cortex) of the kidney. (D) Western blot analysis of glomerular cell lysates obtained from two $FAK^{fl/fl}$;*Pod-Cre* mice and one $FAK^{+/+}$;*Pod-Cre* mouse immunoblotted with α-FAK and α-β-actin. (E) Representative Western blot from two $FAK^{fl/fl}$;*Pod-Cre* mouse primary podocytes (left two lanes) and two $FAK^{+/+}$;*Pod-Cre* mice (two right lanes) immunoblotted with α-FAK, α-podocin, and α-paxillin.

were born in the expected Mendelian frequency, comprising 19% of the offspring (26 of 140). To confirm specificity, we conducted PCR analysis of DNA from the kidney, liver, and heart, which revealed that *FAK* had been deleted in cells from the kidney but not in other organs (Figure 2C). Western blot analysis of glomerular cell lysates harvested by Dynalbeads demonstrated markedly diminished FAK expression in the $FAK^{fl/fl}$;*Pod-Cre* mice (Figure 2D). Because a faint band most likely represented FAK expression in mesangial and endothelial cells in the glomerular cell lysates, primary podocytes were isolated (Supplemental Figure 1) and further confirmed the loss of FAK expression in the podocytes from $FAK^{fl/fl}$;*Pod-Cre* mice (Figure 2E). The decrease in FAK expression did not affect expression of focal adhesion molecules, paxillin (Figure 2E), Crk, or vinculin (data not shown).

Deletion of FAK in Podocytes Does not Affect Baseline Proteinuria or Renal Function

The $FAK^{fl/fl}$;*Pod-Cre* pups were born and seemed to grow and behave normally into adulthood. At 6 months of age, there were no significant differences between the $FAK^{fl/fl}$;*Pod-Cre* and $FAK^{+/+}$;*Pod-Cre* mice in regard to body weight, plasma, and urine electrolytes and blood urea nitrogen (data not shown). Renal histology revealed no obvious abnormalities in glomerular architecture or morphology (Supplemental Figure 2A), and no increase in interstitial fibrosis was detected on Trichrome-stained sections (data not shown). Urine from $FAK^{fl/fl}$;*Pod-Cre* and $FAK^{+/+}$;*Pod-Cre* mice obtained at ages 2, 4, 6, 8, 10, and 26 weeks and analyzed by ELISA quantification and standardized to the urinary creatinine demonstrated no difference in albumin-creatinine ratio (ACR) between $FAK^{fl/fl}$;*Pod-Cre* and $FAK^{+/+}$;*Pod-Cre* mice (Supplemental Figure 2B).

Proteinuria and Podocyte Effacement Are Reduced in $FAK^{fl/fl}$;*Pod-Cre* Mice after Podocyte Injury

As LPS and rabbit anti-mouse GBM—induced glomerular injury resulted in robust FAK activation within the glomerulus (Figure 1D), we next explored the potential effect after the loss of podocyte FAK expression and activation on proteinuria induced by these models. After LPS injection, there was a significant decrease in the ACR in the $FAK^{fl/fl}$;*Pod-Cre* mice compared with $FAK^{+/+}$;*Pod-Cre* mice (37 ± 8 *versus* 177 ± 21 μg/mg at 24 hours, ranging from 12 to 72 hours; Figure 3A). Primary podocyte cell lysates harvested by Dynalbeads from $FAK^{fl/fl}$;*Pod-Cre* mice revealed loss of FAK activation with or without LPS (Figure 3B). Because albuminuria was significantly reduced in the $FAK^{fl/fl}$;*Pod-Cre* mice after LPS treatment, we next examined podocyte ultrastructure. As expected, podocytes from $FAK^{+/+}$;*Pod-Cre* mice demonstrated foot process effacement, which was significantly reduced in the $FAK^{fl/fl}$;*Pod-Cre* mice (Figure 3C). The average number of foot processes per unit length of basement membrane was reduced by 2.2-fold in $FAK^{+/+}$;*Pod-Cre* mice when compared with $FAK^{fl/fl}$;*Pod-Cre* mice after LPS treatment (Figure 3D). Because another rodent model inducing murine glomerulonephritis also demonstrated FAK activation in the $FAK^{+/+}$;*Pod-Cre* mice, we next performed experiments to determine the effect of rabbit anti-mouse GBM antibody in $FAK^{fl/fl}$;*Pod-Cre* mice. FAK activation within the podocytes was again significantly diminished in these mice after administration of rabbit anti-

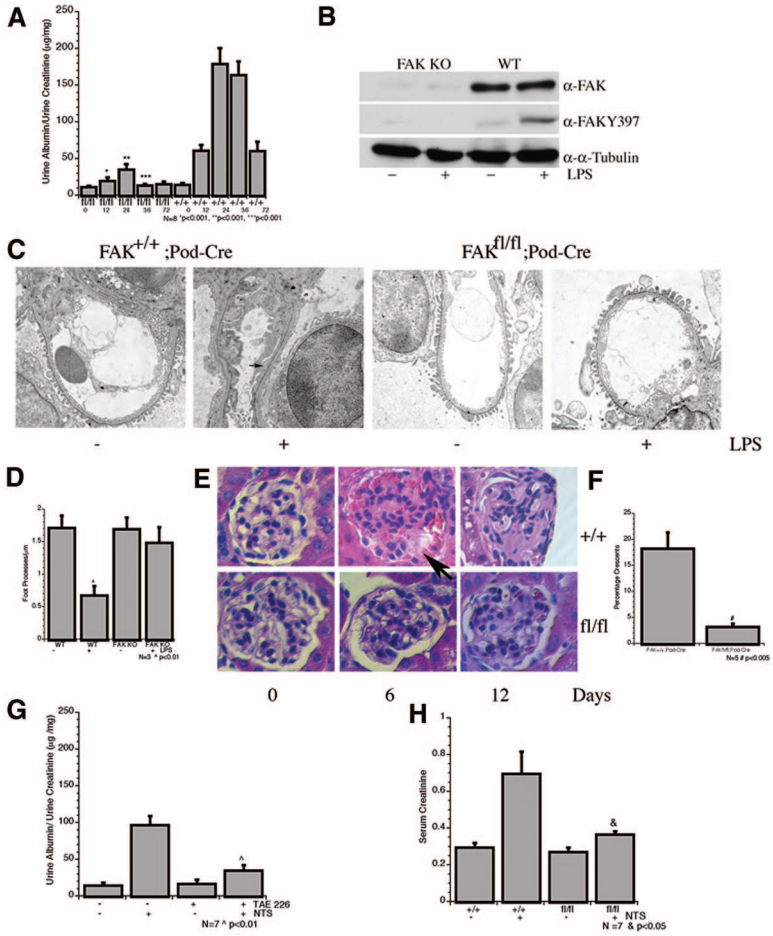

Figure 3. Deletion of FAK in podocytes diminishes podocyte injury and proteinuria. (A) ACR from *FAK*$^{fl/fl}$*;Pod-Cre* and *FAK*$^{+/+}$*;Pod-Cre* mice after LPS at indicated time points. ACR measured from samples at 0, 12, 24, 36, and 72 hours ($n = 8$). *$P < 0.001$ at 12 hours; **$P < 0.001$ at 24 hours; ***$P < 0.001$ at 36 hours. (B) Representative Western blot from isolated primary podocyte cell lysates from *FAK*$^{fl/fl}$*;Pod-Cre* and *FAK*$^{+/+}$*;Pod-Cre* mice stimulated with or without LPS and immunoblotted with α-FAK, α-pFAK 397, and α-α-tubulin. (C) Representative electron microscopy image of *FAK*$^{fl/fl}$*; Pod-Cre* and *FAK*$^{+/+}$*;Pod-Cre* mouse podocytes stimulated with or without LPS. (D) Quantification of C ($n = 3$). ^$P < 0.01$. (E) Representative hematoxylin and eosin staining of glomeruli from *FAK*$^{+/+}$*;Pod-Cre* and *FAK*$^{fl/fl}$*;Pod-Cre* mouse after rabbit anti-mouse GBM treatment at the indicated time points. (F) Quantification of glomerular crescent formation (expressed as percentage of 25 glomeruli examined per mouse) ($n = 5$, #$P < 0.005$). (G) ACR at day 6 after injection of α-rabbit-anti-mouse GBM in *FAK*$^{fl/fl}$*;Pod-Cre* and *FAK*$^{+/+}$*;Pod-Cre* mice ($n = 7$). ^$P < 0.01$. (H) Serum creatinine at day 6 after injection of α-rabbit-anti-mouse GBM in *FAK*$^{fl/fl}$*;Pod-Cre* and *FAK*$^{+/+}$*;Pod-Cre* mice ($n = 7$). &$P < 0.05$.

mouse GBM antibody, although linear IgG staining was observed equally along the GBM in both *FAK*$^{fl/fl}$*;Pod-Cre* and *FAK*$^{+/+}$*;Pod-Cre* glomeruli (data not shown). In the *FAK*$^{fl/fl}$*; Pod-Cre* mice, there was diminished crescent formation (3.4 ± 0.4 *versus* 18.3 ± 4.3%; Figure 3, E and F), albuminuria (90 ± 12 μg/mg in *FAK*$^{+/+}$*;Pod-Cre versus* 25 ± 4 μg/mg in *FAK*$^{fl/fl}$*; Pod-Cre* mice; Figure 3G), and protection from acute renal failure assessed by serum creatinine (0.70 ± 0.12 mg/dl in *FAK*$^{+/+}$*; Pod-Cre versus* 0.37 ± 0.02 mg/dl in *FAK*$^{fl/fl}$*;Pod-Cre* mice; Figure 3H) when compared with *FAK*$^{+/+}$*;Pod-Cre* mice.

Podocytes Lacking FAK Expression Exhibit Diminished Cell Spreading and Motility

After podocyte injury, the increase in FAK Y397 phosphorylation may play an integral role in cell movement secondary to focal adhesion turnover, which leads to subsequent effacement of the foot processes, thereby leading to proteinuria. To address the role of FAK in podocyte motility, we generated stable immortalized podocytes expressing micro RNA-adapted short-hairpin RNA (shRNAmir) targeting FAK and demonstrated by Western blot and densitometry to have >80% knockdown (KD) in two different FAK shRNAmir (Supplemental Figure 3A, quantified in Figure 3C). To confirm results obtained from immortalized podocytes, we next harvested glomeruli from *FAK*$^{fl/fl}$*;Pod-Cre* and *FAK*$^{+/+}$*; Pod-Cre* mice using Dynalbeads, which underwent sieving to produce primary podocytes. Western blot analysis demonstrated that FAK activation peaked at 6 hours and diminished by 72 hours after LPS treatment (Figure 4A, quantified in Figure 4B). We next examined adhesion of these primary podocytes by plating them on collagen-coated plates. Experiments revealed that 82% of the cells adhered normally, with no difference in adhesion between the WT and FAK null podocytes (Figure 4C). Next, we assessed podocyte cell spreading by the quantifying the relative surface area after plating with or without LPS for 4 hours. Podocytes lacking FAK resulted in a three-fold reduction in cell spreading when compared with WT podocytes (Figure 4D, quantified in Figure 5B). To assess random podocyte migration, we seeded *FAK*$^{fl/fl}$*; Pod-Cre* or *FAK*$^{+/+}$*;Pod-Cre* podocytes with or without LPS onto Transwell filters. There was a significant increase in migration in the LPS-stimulated podocytes from *FAK*$^{+/+}$*;Pod-Cre* mice, which was significantly reduced in the podocytes from *FAK*$^{fl/fl}$*; Pod-Cre* mice (Figure 4E, quantified in Figure 4F). Similar findings of inhibited migration were also confirmed in the immortalized podocytes expressing FAK shRNAmir after LPS treatment (Supplemental Figure 3D). To determine coordinated sheet migration, we next performed a wound-healing assay on a monolayer of *FAK*$^{fl/fl}$*;Pod-Cre* or *FAK*$^{+/+}$*;Pod-Cre* primary podocytes with or without LPS. In comparison with *FAK*$^{+/+}$*;Pod-Cre* primary podocytes, the *FAK*$^{fl/fl}$*;Pod-Cre* podocytes had a significant decrease in wound closure after LPS treatment (Figure 4G, quan-

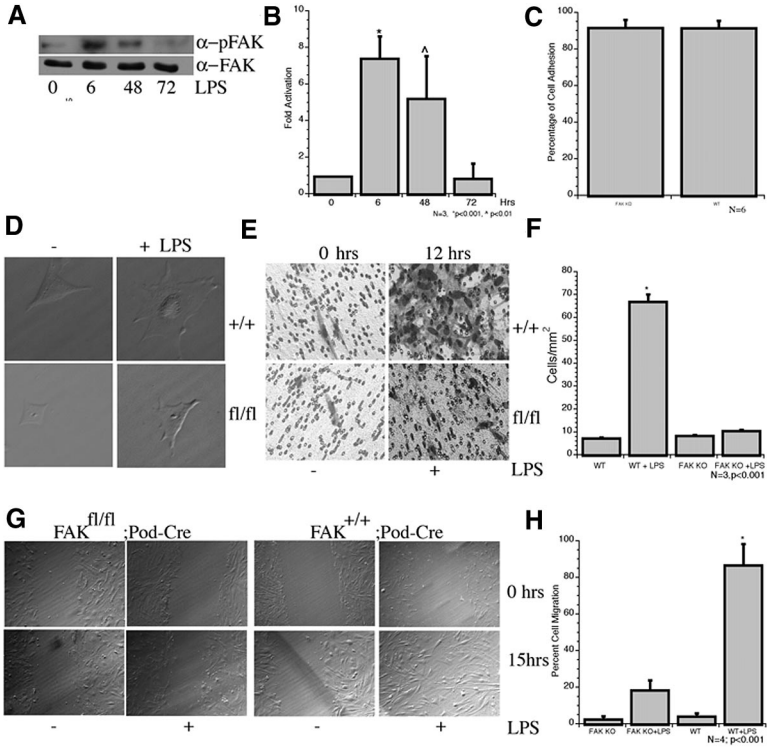

Figure 4. *FAK$^{fl/fl}$;Pod-Cre* mouse primary podocytes are resistant to LPS stimulated migration. (A) Representative Western blot from *FAK$^{+/+}$;Pod-Cre* primary podocytes with or without LPS immunoblotted with α-pFAK Y397 and α-FAK at the indicated time points. (B) Quantification of fold increase by densitometry ($n = 3$). *$P < 0.001$; ^$P < 0.01$. (C) Quantification of adhesion assay ($n = 4$). (D) Representative image of cell spreading of primary *FAK$^{+/+}$;Pod-Cre* and *FAK$^{fl/fl}$;Pod-Cre* podocytes stimulated with or without LPS. (E) Podocytes were pretreated with or without LPS for 6 hours and plated on Transwell filters and allowed to attach for 6 hours, and cells that had migrated to the bottom of the Transwell in 12 hours were photographed. Cell migration was scored positive when the nuclei were visible. (F) Quantification of E ($n = 3$). *$P < 0.001$ *FAK$^{+/+}$;Pod-Cre* (WT) *versus FAK$^{fl/fl}$;Pod-Cre* (FAK null) + LPS. (G) Wound-healing assay from podocytes isolated in *FAK$^{fl/fl}$;Pod-Cre* and *FAK$^{+/+}$;Pod-Cre* mice with or without LPS. (H) Quantification of G ($n = 4$). *$P < 0.001$ *FAK$^{+/+}$;Pod-Cre* (WT) *versus FAK$^{fl/fl}$;Pod-Cre* (FAK null) + LPS. Magnifications: ×200 in D; ×400 in G.

tified in Figure 4H). Finally, to determine that the specific loss of FAK resulted in reduced migration, we re-expressed human FAK, which lacks the mouse FAK shRNAmir sequence (TRCN0000023484) using lentiviral infection into the stable FAK KD podocytes. Successful reconstitution of FAK (FAK RC) resulted in increased cell migration through the Transwell, similar to WT podocytes (Supplemental Figure 3D, quantified in 3E).

FAK Inhibitor TAE-226 Inhibits FAK Activation and Podocyte Migration

Because FAK deletion in podocytes seems to reduce injury, proteinuria *in vivo*, and podocyte cell spreading and motility *in vitro*, we next determined the possible therapeutic role of inhibiting FAK by using the FAK inhibitor TAE-226 (Novartis Pharmaceuticals), an agent currently under investigation for treatment of various malignancies.[19,21,31] Primary WT podocytes pretreated with TAE-226 with or without LPS resulted in reduced FAK activation (Figure 5A). Cell spreading was assessed in primary WT podocytes pretreated with or without TAE-226 and with or without LPS. WT podocytes that had been pretreated with TAE-226 resulted in diminished cell spreading similar to what was quantified in the FAK null podocytes (Figure 5B). To determine individual and sheet migration, podocytes that were pretreated with TAE-226 before LPS demonstrated significantly diminished migration (Figure 5C, quantified in Figure 5D; Figure 5E, quantified in Figure 5F), which recapitulated the findings of our FAK null and FAK knockdown podocytes. Immortalized podocytes subjected to treatment with TAE-226 with or without LPS also revealed significantly reduced cell migration through Transwell Filters (data not shown).

Loss of FAK Activation Results in Diminished Matrix Metalloproteinase 2 Activity

To evaluate further the mechanism involved in preventing LPS-induced migration of FAK KD and FAK null podocytes, we assessed downstream signaling events regulated by FAK. One target is the matrix metalloproteinase (MMP) family, which constitutes more than 25 secreted and cell surface enzymes that process or degrade numerous substrates.[32] It has been demonstrated in malignant cancer cells and endothelial cells that FAK activation can induce MMP-2 and -9 activity, which results in increased cell migration.[33–35] Hence, we performed a zymogram to determine MMP-2 activity. After LPS stimulation, there was increased MMP-2 activity in WT podocytes, which was abrogated in the FAK shRNAmir–expressing podocytes, as well as in podocytes pretreated with TAE-226 (Supplemental Figure 4, A and B). A time course revealed that MMP-2 activity after LPS stimulation was maximal at 48 hours in WT podocytes (Supplemental Figure 4C); however, after LPS stimulation, no differences were observed in MMP-9 activity (data not shown). In addition, there was no difference in MMP-2 protein expression by Western blot in both FAK KD and WT podocytes (data not shown). Because tissue inhibitor of metalloproteinase 2 (TIMP-2) is widely known to inhibit MMP-2 and -9 activities, we next performed quantitative PCR (qPCR) on FAK shRNAmir and WT podocytes. Podocytes with diminished FAK expression revealed an eightfold increase in expression of TIMP-2 (Supplemental Figure 4E). Western blot analysis for TIMP-2 also confirmed the findings of increased

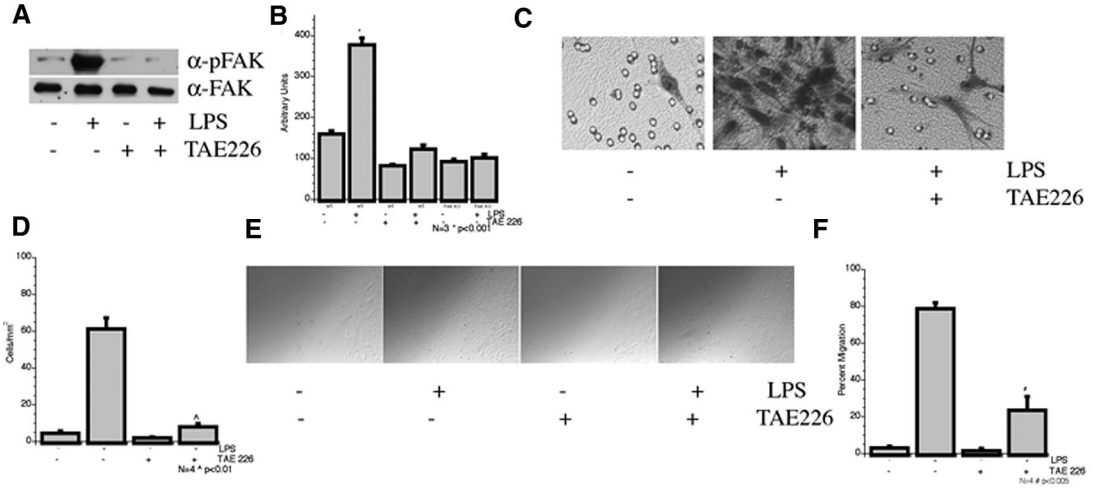

Figure 5. FAK inhibitor TAE-226 inhibits podocyte FAK activation and migration. (A) Primary podocytes treated with or without TAE-226 and with or without LPS immunoblotted with α-FAK and α-pFAK Y397. (B) Quantification of cell-spreading assay in podocytes isolated from $FAK^{fl/fl}$;*Pod-Cre* and $FAK^{+/+}$;*Pod-Cre* mice treated with or without LPS and with or without TAE-226 ($n = 3$). $^{*}P < 0.001$; lane 2 *versus* lane 4 or lane 6. (C) Podocytes treated with or without TAE-226 were seeded on Transwell filters for 6 hours and treated with or without LPS, and cells that migrated to the bottom were photographed. (D) Quantification of C ($n = 4$). $^{\wedge}P < 0.01$. (E) Wound-healing assay from WT primary podocytes treated with or without LPS and with or without TAE-226. (F) Quantification of E ($n = 4$). $^{\#}P < 0.005$. Magnification, ×400.

protein expression from the FAK shRNAmir podocyte cell lysates (Supplemental Figure 4D). To examine further the effect of increased TIMP-2 expression and decreased MMP-2 activity in the FAK shRNAmir cell lines, we generated TIMP-2-shRNAmir and injected them into FAK shRNAmir–expressing cells. Podocytes with knockdown of TIMP-2 alone or both FAK and TIMP-2 demonstrated significant knockdown of TIMP-2 mRNA expression (Supplemental Figure 4E). Conversely, after LPS stimulation, zymography revealed MMP-2 activity had been partially restored in the FAK + TIMP-2 shRNAmir–expressing cells (Supplemental Figure 4F). Next, to determine whether reducing TIMP-2 expression in podocytes stably expressing FAK shRNAmir would increase cell migration, we performed Transwell assay. Results demonstrated that reducing TIMP-2 expression in FAK KD podocytes partially restored individual cell migration (Supplemental Figure 4G). Last, to determine TIMP-2 expression *in vivo*, we stained kidney cryosections from $FAK^{fl/fl}$;*Pod-Cre* or $FAK^{+/+}$;*Pod-Cre* with α-TIMP-2 antibody, revealing increased cytoplasmic TIMP-2 levels within the glomerulus (Supplemental Figure 4H).

Loss of FAK in Podocytes Results in Maintenance of Actin Stress Fibers and the Sustained Activation of Rho

Rearrangement of the actin cytoskeletal complex also has been demonstrated to play a critical role in foot process effacement.[36] Because FAK null podocytes and WT podocytes pretreated with TAE-226 have significantly delayed cell spreading and migration, we next stained cultured primary podocytes with phalloidin after stimulation with or without LPS (Figure 6A). Even after LPS stimulation, the FAK null podocytes as well as podocytes pretreated with TAE-226 continued to retain their central stress fiber formation. To define this mechanism further, we first examined formation of focal adhesions, which functions as a connection between the cytoskeleton and the extracellular matrix. There was no difference in the level of LPS-induced phosphorylation of paxillin at serine 83, a key regulator of FAK recruitment and activation,[37] between the WT and FAK KD podocytes (Figure 6B). Moreover, because cell spreading by lamellipodial extension has also been shown to correlate with the activation of small-Rho-GTPase-Rac, we next performed a Rac activation assay. Similar to the results of paxillin phosphorylation in FAK KD and WT podocytes, LPS stimulation demonstrated no definable difference in activation between the two cell types (Figure 6C). Previous evidence demonstrated that FAK activation suppresses Rho activity,[38,39] leading to reduced stress fiber formation and increased focal adhesion turnover. Maintenance of Rho activity seems to be critical for proper podocyte stress fiber formation,[40] which led us to determine whether FAK regulates Rho activity in podocytes. Compared with WT podocytes, FAK KD podocytes demonstrated a marked increase in Rho activation, which was sustained after LPS stimulation (Figure 6D). To solidify further that FAK deletion in podocytes results in the maintenance of stress fiber formation, we re-expressed FAK in FAK null podocytes. Re-expression of FAK resulted in loss of stress fiber formation (Figure 6E). To determine whether loss of Rho activation results in reduced stress fiber formation, we pretreated FAK null podocytes with Rho associated kinase inhibitor Y27632 before LPS stimulation. Results demonstrated that there was a significant loss of stress fiber formation (Figure 6E, quantified in Figure 6F) in FAK null

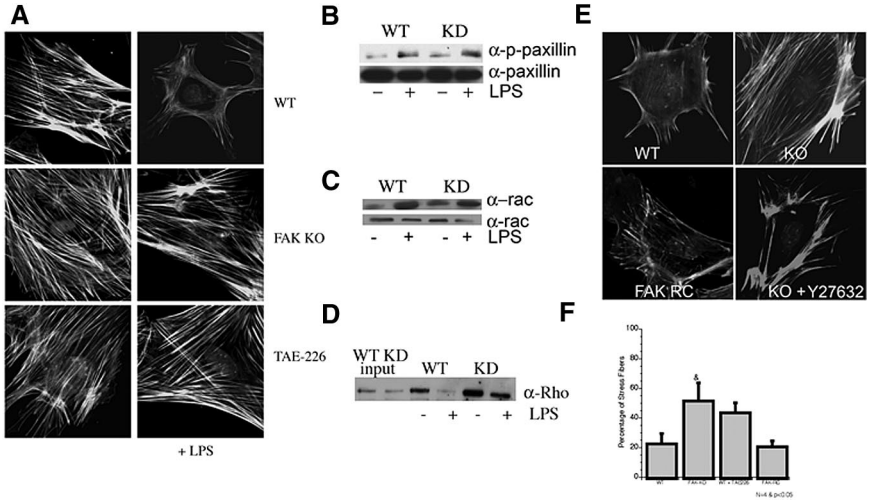

Figure 6. Loss of FAK results in increased stress fiber formation and activation of Rho. (A) Podocytes harvested from isolated glomeruli from *FAK*$^{+/+}$*;Pod-Cre* and *FAK*$^{fl/fl}$*; Pod-Cre* mice (designated as WT, FAK KO, and TAE-226) treated with or without LPS were immunostained with α-phalloidin and TOPRO (nuclear marker). (B) FAK KD and WT immortalized podocytes treated with or without LPS for 6 hours and immunoblotted with α-paxillin and α-p-paxillin (pS83). (C) FAK KD and WT podocytes treated with or without LPS and incubated with agarose-PAK and immunoblotted with α-Rac. (D) FAK KD and WT podocytes treated with or without LPS and incubated with agarose-Rhotekin RBD and immunoblotted with α-Rho. (E) WT, KO, FAK RC, and KO podocytes pretreated with Rho associated kinase inhibitor Y27632 (1 μm) stimulated with LPS were immunostained with α-phalloidin and TOPRO (nuclear marker). (F) Quantification of percentage of stress fiber formation from E after LPS stimulation ($n = 4$). $^{\&}P < 0.05$, lane 2 *versus* lane 4 or 5.

podocytes pretreated with Y27632, which further resulted in increased cell spreading after LPS stimulation, mimicking WT podocytes (data not shown).

FAK Inhibitor TAE-226 Is Protective in Early Glomerular Injury in Rodent Models

Because the conditional podocyte FAK knockout mouse resulted in reduction of albuminuria and podocyte effacement after LPS and rabbit anti-mouse GBM injections, we next pretreated WT mice with TAE-226 (50 mg/kg) before injury. FAK activation within the glomerulus was inhibited in mice that were pretreated with TAE-226 before LPS or rabbit anti-mouse GBM injections (data not shown). Next we assessed the role of TAE-226 in albuminuria after LPS induction (Supplemental Figure 5). Mice pretreated with TAE-226 before injury with LPS exhibited reduced albuminuria measured by ACR (198.2 ± 7.0 *versus* 62.9 ± 6.8 [24 hours] and 130.6 ± 5.9 *versus* 45.2 ± 5.2 [48 hours]; Figure 7A). Furthermore, podocyte effacement was reduced in mice that were pretreated with TAE-226 before LPS induction (Figure 7B, quantified in Figure 7C). Because LPS induces only transient proteinuria, we next used our rabbit anti-mouse GBM model to investigate the role of TAE-226 treatment at the time of injury as well as treatment after injury. Mice that were treated with TAE-226 simultaneously with the induction of rabbit anti-mouse GBM revealed an improvement in proteinuria at day 12 (105.4 ± 11.7 *versus* 37.2 ± 4.2 μg/mg; Figure 7D); however, when mice were treated with TAE-226 after injury had already occurred, no improvement in proteinuria was observed (data not shown). To assess kidney function, we measured serum creatinine in mice pretreated, simultaneously treated, or treated after injury. In mice pretreated with TAE-226, there was a significant reduction in serum creatinine at day 6 (Figure 7E, first three bars), which extended to day 12 with continued treatment (Figure 7E, fourth *versus* fifth bar). In mice that were treated with TAE-226 at the time of injury, there was a modest but significant reduction in serum creatinine when measured at day 12 (Figure 7E, last bar); however, when mice were treated after injury had already occurred, no improvement in serum creatinine was observed (Figure 7F).

DISCUSSION

Because injury to podocytes often leads to foot process effacement with resultant proteinuria and progression to kidney failure, understanding the mechanisms driving this process is critical for developing therapeutic interventions. The available treatment options for glomerular injury are limited to alkylating agents, steroids, and angiotensin-converting enzyme inhibitors and angiotensin receptor blockers.[1,41] Using the established Cre-loxP–based conditional KO approach, we deleted FAK expression specifically in podocytes, which results in decreased podocyte retraction and foot process effacement after injury. To our knowledge, this is the first report to demonstrate a protective role in podocyte effacement by inhibiting FAK activation genetically as well as pharmacologically, when mice are treated either before or at the time of foot process effacement.

We provide evidence that FAK is activated after podocyte injury in mouse models of glomerulopathy (Figure 1D). Increased tyrosine phosphorylation within focal adhesion proteins, increased Pyk2, and FAK activation have been reported in patients with glomerular diseases.[42–44] FAK activation seems to occur early in the disease process after LPS treatment (Figure 1D). We hypothesize that this activation may initiate focal adhesion rearrangement, resulting in the retraction of the foot processes and leading to effacement. When FAK was deleted specifically in podocytes, proteinuria and foot process effacement after glomerular injury were diminished (Figure 3, C and D). Moreover, the cell culture data support the notion that podocytes lacking FAK demonstrate diminished cell spreading and migration after LPS stimulation (Figure 4, D through H). One caveat in these assays is that *in vitro* cell spreading and

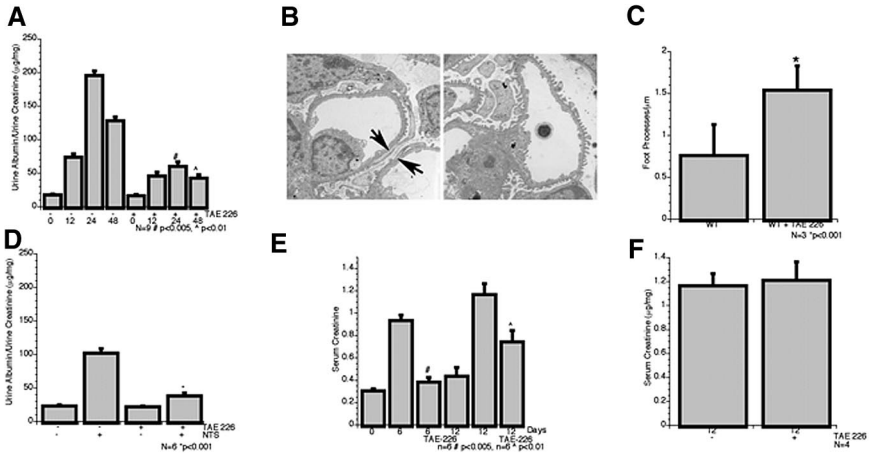

Figure 7. TAE-226 treatment reduces proteinuria and podocyte injury. (A) ACR from mice pretreated with or without TAE-226 and with or without LPS at the indicated time points ($n = 9$). $^{\#}P < 0.005$; $^{\wedge}P < 0.01$. (B) Representative electron microscopy image of WT mice treated with or without TAE-226 and with or without LPS; arrow indicates podocyte effacement (left). (C) Quantification of C ($n = 3$). $P < 0.001$. (D) ACR in mice treated at time of injury with or without TAE 226 and with or without rabbit anti-mouse antibody ($n = 6$). $^{*}P < 0.001$. (E) Serum creatinine obtained from mice pretreated with or without TAE-226, before injection of rabbit anti-mouse GBM antibody (first four bars). Serum creatinine from mice that were treated with or without TAE-226 at the time of injection of rabbit anti-mouse GBM antibody (last two bars; $n = 6$). $^{\#}P < 0.005$; $^{\wedge}P < 0.01$. (F) Serum creatinine from mice treated with or without TAE 226 after injury with rabbit anti-mouse GBM antibody ($n = 4$).

migration may be distinct from podocyte effacement; however, there is a lack of a reliable *in vitro* "read out" assay that resembles what actually may occur *in vivo* during foot process effacement.

Recent studies have also suggested that podocyte movement may be critical for foot process effacement, because loss of uPAR also prevented proteinuria through the inhibition of Rac, a small GTPase, which is important for lamellipodial extension.[22] One hypothesis is that the loss of uPAR may also lead to inhibition of FAK activation, because it has been demonstrated that uPAR is a strong activator of FAK.[45,46] In addition, FAK activation has been shown to promote Rac signaling,[47] which facilitates Rac and p21-activated kinase interactions.[48] Another possible downstream target for FAK signaling is through Crk,[49] because it has been reported that the loss of Crk specifically in podocytes results in inhibition of podocyte injury after protamine sulfate infusion (L.H., personal communication, November 2008). Although we explored these two downstream targets of FAK, we failed to observe a difference in Rac activation between the WT and FAK KD podocytes after LPS treatment (Figure 6C) or Crk protein levels in our FAK KD and null podocytes after LPS treatment (data not shown), suggesting an alternative mechanism.

FAK activation has also been shown to promote metalloproteinase activity.[33,47,50] Indeed, when compared with WT podocytes, there was diminished MMP-2 activity in FAK null and FAK shRNAmir podocytes after LPS treatment. We postulated that the decrease in MMP-2 activity was most likely due to the increased TIMP-2 levels observed in the FAK null and FAK KD podocytes. Moreover, the decrease in FAK KD and null podocytes to spread and migrate after LPS may be due to the elevated basal Rho activation in these cells, resulting in the maintenance of stress fibers.

Because FAK inhibitors are available and are currently being tested for treatment of malignancies,[18–21] the possibility to test these compounds in human glomerular diseases is also quite attractive. Pretreatment with the FAK inhibitor TAE-226 resulted in the reduction of proteinuria after injury in our mouse models, and concurrent treatment also demonstrated a reduction in proteinuria and kidney injury; however, when TAE-226 was given after severe injury had already occurred, no improvement in kidney function was observed. We postulate that treatment with TAE-226 after foot process effacement has already occurred may actually hinder the restoration to normal podocyte morphology, because focal adhesion turnover may also be required for this process.

Collectively, the results of this study allow us to define the possible pathogenic role of FAK activation after podocyte injury in two independent models and through the availability of FAK inhibitors may allow for future therapeutic options in humans. These findings motivate further studies for investigating FAK, as well as other targets important for cell spreading and migration, thereby giving us a better understanding of the specific signaling events that are required for podocyte effacement.

CONCISE METHODS

Creation and Genotyping of Conditional FAK Knockout Mice

FAK$^{fl/+}$ mice (129 SVJ × C57BL/6) were generated as described previously.[29,30] Podocin-Cre mice (C57BL/6 × SJL) were obtained from Dr. Larry Holzman.[24] Tail genotyping was performed using FAK primer 5′-AGGGCTGGTCTGCGCTGACAGG-3′ and reverse primer 5′-GCTGATGTCCCAAGCTATTCC-3′. The expected sizes of WT allele, floxed allele, and deleted allele were 1600, 1500, and 600 bp, respectively. To determine Cre expression, we used FAK primer 5′-ACAGCTCCACCAAGACACAG-3′ and reverse primer 5′-TCCGGTTATTCAACTTGCACC-3′ to generate a 400-bp fragment.

LPS-Induced Podocyte Injury and Treatment with TAE-226

All animal studies were approved by Yale Institutional Animal Care and Use Committee. Female (6 to 8 weeks of age), *FAK*$^{fl/fl}$;*Pod-Cre* mice and *FAK*$^{+/+}$;*Pod-Cre* mice were used for these experiments.

Baseline urine albumin excretion was measured as per the manufacturer's protocol using ELISA Albumin Kit (Bethyl Laboratories) and standardized to urine creatinine, before animals were administered an intraperitoneal injection with or without 200 μg of LPS (InvivoGen) in a total volume of 200 μl of sterile PBS.[25] Urinary albumin excretion was measured at various time points, and kidneys were harvested and processed for hematoxylin and eosin and immunofluorescence staining. FAK primer effacement was assessed by transmission electron microscopy and evaluated in a blinded manner by J.C. TAE-226 (Novartis Pharmaceuticals) was gavaged (50 mg/kg) in 200 μl of 0.5% methylcellulose starting 5 days before LPS injection and continued until mice were killed.

Rabbit Anti-GBM–Induced Podocyte Injury

Rabbit anti-mouse GBM antibody (nephrotoxic serum) was generated by Lampire Biologic Laboratories. Sera were obtained from the rabbits 2 months after immunization of glomeruli. Preimmune rabbit serum was used as a negative control. *FAK $^{fl/fl}$;Pod-Cre* mice and *FAK$^{+/+}$;Pod-Cre* mice were used for these experiments. Briefly, 8- to 16-week-old mice were immunized with an intraperitoneal injection of 200 μg of rabbit IgG (Jackson Immunoresearch Laboratories) in 200 μg of a 1:1 emulsion with complete Freund's adjuvant (Sigma Chemical Co., St. Louis, MO). Six days later (day 0), glomerulonephritis was induced with an intravenous injection of 200 μl of a 1:3 dilution of rabbit anti-mouse GBM serum.[26,27] Urinary albumin was determined by ELISA (Bethyl Laboratories), and serum creatinine was evaluated on days 6 and 12. TAE-226 (50 mg/kg) was gavaged 5 days before and continued up to 12 days after induction of glomerulonephritis. In another set of experiments, TAE-226 was started the same day as induction of glomerulonephritis and followed for 12 days. In the last set of experiments, TAE-226 was started 6 days after induction of glomerulonephritis.

Podocyte Cell Culture and Reagents

Conditionally immortalized mouse podocyte clone was provided by Dr. Stuart Shankland (University of Washington, Seattle, Washington). The preparation and characterization of these cells has been described in detail elsewhere. Podocytes were maintained in RPMI 1640 medium (21870-076; Life Technologies BRL, Gaithersburg, MD) supplemented with 9% FCS (Life Technologies BRL), 2 mM L-glutamine (9317; Irvine Scientific), 0.01 M HEPES (H0887; Sigma), 0.075% sodium bicarbonate (S8761; Sigma) and sodium pyruvate, 100 U/ml penicillin, and 100 μg/ml streptomycin in a humidified atmosphere with 5% CO_2. For propagation of podocytes, the culture medium was supplemented with 50 U/ml recombinant mouse γ-IFN (311797200; Roche) to enhance the expression of large T-antigen, and the cells were cultured at 33°C (permissive conditions) on type I collagen–coated (354231; BD Biosciences, San Jose, CA) dishes. The cells were cultured at 37°C (nonpermissive conditions) to induce differentiation without γ-IFN. It took 12 to 14 days to induce differentiation.[51] Podocytes between passages 16 and 25 were used in all experiments. For primary podocytes, glomeruli were harvested using Dynal beads as described previously,[52,53] and glomeruli were passed through a 100-μm cell strainer (BD Biosciences) and plated on type 1 collagen-coated plates at 37°C. Subculture was performed by detaching with trypsin-EDTA and passing through 40-μm cell strainer (BD Biosciences) and cultured on collagen I–coated dishes.[54] Purity was determined to be 97.5% (co-staining WT-1 [podocyte-specific marker with DAPI]), and qPCR was performed with podocin (specific for podocytes; primer forward 5′-CTGTCCAGCTTCGATACTTGC-3′, reverse 5′-GGTTTGGAGGAACTTGGGTAG-3′) and Thy-1 (specific for mesangial cells; primer forward 5′-CGCTCTCCTGCTCTCAGTCT-3′ and reverse 5′-AGGCTGAACTCATGCTGGAT-3′). The antibodies utilized are: anti–TIMP-2, anti–α-tubulin, and anti–WT-1 (Santa Cruz Biotechnology); anti-FAK, anti-paxillin, and anti-Crk (BD Transduction); anti–phospho-FAK against tyrosine 397 (Chemicon); anti-podocin (Sigma); anti–phospho-paxillin S83 (generated by Dr. Lloyd Cantley); anti-Rac and anti-Rho (Millipore); and anti-nephrin (provided by L.H. and Dr. David Salant).

Subcloning and Generation of Stable Cell Lines

The shRNAmir encoded in a pLKO.1 vector targeting FAK hairpin sequence (TRCN0000023484 and TRCN0000023486) and TIMP-2 (TRCN0000071949) were purchased from Open Biosystems and transfected with Lipofectamine 2000 into 293FT cells together with two packaging vectors, pCMVΔR8.91 and pMD.G. The supernatant was filtered (0.45 μm), and undifferentiated podocytes were infected, followed by the addition of puromycin 1 μg/ml to lentiviral-treated and control podocytes to generate stable cell lines. A scramble shRNAmir (Open Biosystems) served as a negative control.

For FAK overexpression, the FAK fragment was obtained by performing PCR on pCMV.SPORT6-PTK2 (ATCC), using primers 5′-CGCGGATCCATGGCAGCTGCTTACCTTGAC-3′ and 5′-AAGGAAAAAAGCGGCCGCTCAGTGTGGTCTCGTCTGCC-3′, then subcloned into the lentivirus-derived vector pLEX-MCS (Open Biosystems) using NotI and BamHI sites.

Adhesion, Spreading, Transwell, and Wound-Healing Migration Assay

For podocyte adhesion, pass 1, primary FAK null and WT podocytes isolated from Dynalbeads were trypsinized and counted by hemocytometer, and 300 cells were plated on collagen I–coated 48-well plates for 2 hours. Cells were washed three times with PBS, and the total number of adherent cells were counted. Each well represented an *n* of 1, and data are reported as mean ± SEM. For podocyte spreading, primary podocytes as described already were trypsinized and plated on collagen-coated coverslips with or without TAE-226 (10 μM) and stimulated with or without LPS (20 μg) for 4 hours and photographed using Hoffman modulation and Spot RT camera (Diagnostic Instruments). Relative cell area (in square pixels) was determined using NIH image. Transwell cell culture inserts (pore size 5 μm; Costar Corp., Corning, NY) were coated with type I collagen (354231; BD Biosciences), rinsed once with PBS, and placed in RPMI in the lower compartment. For each experiment, the cells were pretreated with or without TAE-226 and with or without LPS (20 μg) for 6 hours. Podocytes (1×10^4) were seeded in the inserts and allowed to migrate for 12 hours while being incubated at 37°C. Nonmigratory cells were removed from the upper surface of the membrane with cotton-tipped applicators, and migrated cells were fixed and stained with HEMA stain set (PROTOCOL) for 15 minutes each and quantified as de-

scribed previously.[37,55] For wound healing, confluent monolayer of primary or immortalized differentiated podocytes was scraped with a 20-μl pipette followed by stimulation with or without LPS and visualized at 12 hours using Hoffman modulation ($\times$10) and a Spot RT camera (Diagnostic Instruments). Percentage of wound closure was calculated using NIH image: [(Area $T_{12\ hours}$ − Area T_0)/AreaT_0)].

Gelatin Zymography

MMP-2 enzyme activity in the conditioned medium or lysates obtained from differentiated podocytes was monitored by gelatin zymography. Briefly, immortalized podocytes grown in nonpermissive conditions were placed in FCS-free medium containing 0.1% BSA, and condition medium was collected and centrifuged. For gelatin zymography, 25 μl of the twofold concentrated conditioned medium was mixed with 2$\times$ nonreducing sample buffer (125 mmol/L Tris-HCl [pH 6.8], 4% SDS, 40% glycerol, and 0.005% bromophenol blue), incubated for 10 minutes at room temperature, then separated in 7.5% polyacrylamide SDS gel containing 1 mg/ml gelatin. After electrophoresis, the gels were denatured in 2.5% Triton X-100 for 30 minutes, equilibrated in developing buffer (50 mmol/L Tris-HCl buffer [pH 7.5], 0.2 mol/L NaCl, 5 mmol/L $CaCl_2$, and 0.2% Brij-35) for 30 minutes followed by incubation in developing buffer at 37°C for 18 hours. Gels were stained with 0.5% Bright blue R-250 for 30 minutes, washed, destained with destaining solution (methanol:acetic acid:water 50:10:40), and quantified using NIH image.

Protein Isolation and Western Analysis

Podocytes were lysed with a buffer containing 20 mM Tris-HCl (pH 7.5), 150 mM NaCl, 1 mM Na_2EDTA, 1 mM EGTA, 1% Triton, 2.5 mM sodium pyrophosphate, 1 mM β-glycerophosphate, a protease inhibitor cocktail (Sigma-Aldrich P8340), and Phosphatase Inhibitor Cocktail 2 (Sigma-Aldrich P5726). After determination of protein concentration, 40 μg of protein per sample was separated by SDS-PAGE, electrophoretically transferred to Immobilon-P membranes (Millipore, Billerica, MA), immunoblotted with the appropriate antibody, and visualized by enhanced chemiluminescence (Amersham Biosciences, Pittsburgh, PA) as described previously.[56]

qPCR Analysis

Two-step qPCR was performed to determine gene expression from cultured podocytes. Total RNA was extracted using the RNeasy Kit (Qiagen), and 1 μg of RNA was reverse-transcribed using random hexamer primers according to the manufacturer's instructions (iScript cDNA Synthesis Kit; Bio-Rad). qPCR was conducted using power SYBR green mix (Applied Biosystems, Foster City, CA) with a 7300 AB Real-time PCR machine (Applied Biosystems). Primer pairs were selected for their specificity and efficiency: TIMP-2 (forward 5′-CCCATGATCCTTGCTACAT-3′ and reverse 5′-GGGTCCTC-GATGTCAAGAAA-3′) and glyceraldehyde-3-phosphate dehydrogenase (forward 5′-GACCCCTTCATTGACCTCAAC and reverse 5′-CTTCTCCATGGTGGTGAAGA). Target gene expression levels were determined by the comparative threshold cycle (dCt) method, and mRNA ratios are given by 2^{-dCT}. PCR controls run in absence of template were constantly negative.

Kidney Histology and Immunofluorescence and Quantification

Briefly, mice were anesthetized by intraperitoneal injection of ketamine and xylazine followed by perfusion fixation with 40 ml of 4% PFA for immunofluorescence or Karnovsky's solution for electron microscopy experiments. The kidneys were frozen, sectioned at 4 μm, and subjected to antigen retrieval (Retrievagen; BD Biosciences) followed by blocking with 5% BSA for 1 hour. Immunostaining was performed with the appropriate primary antibody overnight at 4°C and secondary antibody at room temperature for 1 hour for visualization. 4,6,-Diamidino-2-phenylindole (DAPI) was included in the mounting medium as a counter stain (Vector Laboratories, Burlingame, CA). For kidney histology, mice were perfusion-fixed as already described followed by sections stained with hematoxylin and eosin or Trichrome or electron microscopy by the Yale Pathology Department. Cultured podocytes were fixed in 4% paraformaldehyde in PBS, permeabilized with 0.5% Triton in PBS for 10 minutes at 4°C, blocked, and then incubated with the appropriate primary and secondary antibodies as described already. Images were obtained either with an epifluorescence confocal laser microscope (FV1000; Olympus) or a Nikon TE2000U inverted microscope equipped with widefield fluorescence. For quantitative analysis of electron microscopy, images were processed in Image J. The number of podocyte foot processes present in each micrograph was divided by the total length of the GBM regions in each image to determine the average density of podocyte foot processes. The percentage of glomeruli, which contains crescents, was assessed in 25 random glomeruli from *FAK$^{fl/fl}$;Pod-Cre* and *FAK$^{+/+}$;Pod-Cre* mice in five separate experiments.

Rac and Rho Activation Assay

FAK KD and FAK WT immortalized podocytes were lysed as per the manufacturer's protocol (Millipore) after simulation with or without LPS (20 μg) and incubated with PAK-agarose (which binds only to RAC-GTP) or Rhotekin-agarose (which binds only Rho-GTP) for 2 hours followed by separation by SDS-PAGE and immunoblotting with the appropriate primary and secondary antibodies.

Statistical Analysis

Plasma and urine electrolytes were analyzed using the Yale University School of Medicine O'Brien Center Physiology Core. The data are expressed as means ± SEM. Statistical significance was determined using the *t* test.

ACKNOWLEDGMENTS

This work was funded by the National Institutes of Health O'Brien Center Pilot and Feasibility Award (S.I.).

We thank Dr. Lloyd Cantley for helpful discussions.

DISCLOSURES

None.

REFERENCES

1. Wiggins RC: The spectrum of podocytopathies: A unifying view of glomerular diseases. *Kidney Int* 71: 1205–1214, 2007
2. Shankland SJ: The podocyte's response to injury: Role in proteinuria and glomerulosclerosis. *Kidney Int* 69: 2131–2147, 2006
3. Ruotsalainen V, Ljungberg P, Wartiovaara J, Lenkkeri U, Kestila M, Jalanko H, Holmberg C, Tryggvason K: Nephrin is specifically located at the slit diaphragm of glomerular podocytes. *Proc Natl Acad Sci U S A* 96: 7962–7967, 1999
4. Patrakka J, Kestila M, Wartiovaara J, Ruotsalainen V, Tissari P, Lenkkeri U, Mannikko M, Visapaa I, Holmberg C, Rapola J, Tryggvason K, Jalanko H: Congenital nephrotic syndrome (NPHS1): Features resulting from different mutations in Finnish patients. *Kidney Int* 58: 972–980, 2000
5. Tryggvason K, Patrakka J, Wartiovaara J: Hereditary proteinuria syndromes and mechanisms of proteinuria. *N Engl J Med* 354: 1387–1401, 2006
6. Mundel P, Heid HW, Mundel TM, Kruger M, Reiser J, Kriz W: Synaptopodin: An actin-associated protein in telencephalic dendrites and renal podocytes. *J Cell Biol* 139: 193–204, 1997
7. Shih NY, Li J, Karpitskii V, Nguyen A, Dustin ML, Kanagawa O, Miner JH, Shaw AS: Congenital nephrotic syndrome in mice lacking CD2-associated protein. *Science* 286: 312–315, 1999
8. Boute N, Gribouval O, Roselli S, Benessy F, Lee H, Fuchshuber A, Dahan K, Gubler MC, Niaudet P, Antignac C: NPHS2, encoding the glomerular protein podocin, is mutated in autosomal recessive steroid-resistant nephrotic syndrome. *Nat Genet* 24: 349–354, 2000
9. Dai C, Stolz DB, Bastacky SI, St-Arnaud R, Wu C, Dedhar S, Liu Y: Essential role of integrin-linked kinase in podocyte biology: Bridging the integrin and slit diaphragm signaling. *J Am Soc Nephrol* 17: 2164–2175, 2006
10. El-Aouni C, Herbach N, Blattner SM, Henger A, Rastaldi MP, Jarad G, Miner JH, Moeller MJ, St-Arnaud R, Dedhar S, Holzman LB, Wanke R, Kretzler M: Podocyte-specific deletion of integrin-linked kinase results in severe glomerular basement membrane alterations and progressive glomerulosclerosis. *J Am Soc Nephrol* 17: 1334–1344, 2006
11. Schaller MD, Hildebrand JD, Shannon JD, Fox JW, Vines RR, Parsons JT: Autophosphorylation of the focal adhesion kinase, pp125FAK, directs SH2-dependent binding of pp60src. *Mol Cell Biol* 14: 1680–1688, 1994
12. Webb DJ, Donais K, Whitmore LA, Thomas SM, Turner CE, Parsons JT, Horwitz AF: FAK-Src signalling through paxillin, ERK and MLCK regulates adhesion disassembly. *Nat Cell Biol* 6: 154–161, 2004
13. Abbi S, Guan JL: Focal adhesion kinase: Protein interactions and cellular functions. *Histol Histopathol* 17: 1163–1171, 2002
14. Schlaepfer DD, Mitra SK, Ilic D: Control of motile and invasive cell phenotypes by focal adhesion kinase. *Biochim Biophys Acta* 1692: 77–102, 2004
15. Calalb MB, Polte TR, Hanks SK: Tyrosine phosphorylation of focal adhesion kinase at sites in the catalytic domain regulates kinase activity: A role for Src family kinases. *Mol Cell Biol* 15: 954–963, 1995
16. Mitra SK, Hanson DA, Schlaepfer DD: Focal adhesion kinase: In command and control of cell motility. *Nat Rev Mol Cell Biol* 6: 56–68, 2005
17. Ilic D, Furuta Y, Kanazawa S, Takeda N, Sobue K, Nakatsuji N, Nomura S, Fujimoto J, Okada M, Yamamoto T: Reduced cell motility and enhanced focal adhesion contact formation in cells from FAK-deficient mice. *Nature* 377: 539–544, 1995
18. Halder J, Lin YG, Merritt WM, Spannuth WA, Nick AM, Honda T, Kamat AA, Han LY, Kim TJ, Lu C, Tari AM, Bornmann W, Fernandez A, Lopez-Berestein G, Sood AK: Therapeutic efficacy of a novel focal adhesion kinase inhibitor TAE226 in ovarian carcinoma. *Cancer Res* 67: 10976–10983, 2007
19. Golubovskaya VM, Virnig C, Cance WG: TAE226-induced apoptosis in breast cancer cells with overexpressed Src or EGFR. *Mol Carcinog* 47: 222–234, 2008
20. Parsons JT, Slack-Davis J, Tilghman R, Roberts WG: Focal adhesion kinase: Targeting adhesion signaling pathways for therapeutic intervention. *Clin Cancer Res* 14: 627–632, 2008
21. Lim ST, Mikolon D, Stupack DG, Schlaepfer DD: FERM control of FAK function: Implications for cancer therapy. *Cell Cycle* 7: 2306–2314, 2008
22. Wei C, Moller CC, Altintas MM, Li J, Schwarz K, Zacchigna S, Xie L, Henger A, Schmid H, Rastaldi MP, Cowan P, Kretzler M, Parrilla R, Bendayan M, Gupta V, Nikolic B, Kalluri R, Carmeliet P, Mundel P, Reiser J: Modification of kidney barrier function by the urokinase receptor. *Nat Med* 14: 55–63, 2008
23. Igarashi P: Kidney-specific gene targeting. *J Am Soc Nephrol* 15: 2237–2239, 2004
24. Moeller MJ, Sanden SK, Soofi A, Wiggins RC, Holzman LB: Podocyte-specific expression of cre recombinase in transgenic mice. *Genesis* 35: 39–42, 2003
25. Reiser J, von Gersdorff G, Loos M, Oh J, Asanuma K, Giardino L, Rastaldi MP, Calvaresi N, Watanabe H, Schwarz K, Faul C, Kretzler M, Davidson A, Sugimoto H, Kalluri R, Sharpe AH, Kreidberg JA, Mundel P: Induction of B7–1 in podocytes is associated with nephrotic syndrome. *J Clin Invest* 113: 1390–1397, 2004
26. Moeller MJ, Soofi A, Hartmann I, Le Hir M, Wiggins R, Kriz W, Holzman LB: Podocytes populate cellular crescents in a murine model of inflammatory glomerulonephritis. *J Am Soc Nephrol* 15: 61–67, 2004
27. Le Hir M, Keller C, Eschmann V, Hahnel B, Hosser H, Kriz W: Podocyte bridges between the tuft and Bowman's capsule: An early event in experimental crescentic glomerulonephritis. *J Am Soc Nephrol* 12: 2060–2071, 2001
28. Xie C, Zhou XJ, Liu X, Mohan C: Enhanced susceptibility to end-organ disease in the lupus-facilitating NZW mouse strain. *Arthritis Rheum* 48: 1080–1092, 2003
29. Peng X, Kraus MS, Wei H, Shen TL, Pariaut R, Alcaraz A, Ji G, Cheng L, Yang Q, Kotlikoff MI, Chen J, Chien K, Gu H, Guan JL: Inactivation of focal adhesion kinase in cardiomyocytes promotes eccentric cardiac hypertrophy and fibrosis in mice. *J Clin Invest* 116: 217–227, 2006
30. Shen TL, Park AY, Alcaraz A, Peng X, Jang I, Koni P, Flavell RA, Gu H, Guan JL: Conditional knockout of focal adhesion kinase in endothelial cells reveals its role in angiogenesis and vascular development in late embryogenesis. *J Cell Biol* 169: 941–952, 2005
31. Slack-Davis JK, Martin KH, Tilghman RW, Iwanicki M, Ung EJ, Autry C, Luzzio MJ, Cooper B, Kath JC, Roberts WG, Parsons JT: Cellular characterization of a novel focal adhesion kinase inhibitor. *J Biol Chem* 282: 14845–14852, 2007
32. Sternlicht MD, Werb Z: How matrix metalloproteinases regulate cell behavior. *Annu Rev Cell Dev Biol* 17: 463–516, 2001
33. Jimenez E, Perez de la Blanca E, Urso L, Gonzalez I, Salas J, Montiel M: Angiotensin II induces MMP 2 activity via FAK/JNK pathway in human endothelial cells. *Biochem Biophys Res Commun* 380: 769–774, 2009
34. Lee JW, Kwak HJ, Lee JJ, Kim YN, Lee JW, Park MJ, Jung SE, Hong SI, Lee JH, Lee JS: HSP27 regulates cell adhesion and invasion via modulation of focal adhesion kinase and MMP-2 expression. *Eur J Cell Biol* 87: 377–387, 2008
35. Mon NN, Hasegawa H, Thant AA, Huang P, Tanimura Y, Senga T, Hamaguchi M: A role for focal adhesion kinase signaling in tumor necrosis factor-alpha-dependent matrix metalloproteinase-9 production in a cholangiocarcinoma cell line, CCKS1. *Cancer Res* 66: 6778–6784, 2006
36. Faul C, Asanuma K, Yanagida-Asanuma E, Kim K, Mundel P: Actin up: Regulation of podocyte structure and function by components of the actin cytoskeleton. *Trends Cell Biol* 17: 428–437, 2007
37. Ishibe S, Joly D, Liu ZX, Cantley LG: Paxillin serves as an ERK-regulated scaffold for coordinating FAK and Rac activation in epithelial morphogenesis. *Mol Cell* 16: 257–267, 2004
38. Ren XD, Kiosses WB, Sieg DJ, Otey CA, Schlaepfer DD, Schwartz MA: Focal adhesion kinase suppresses Rho activity to promote focal adhesion turnover. *J Cell Sci* 113: 3673–3678, 2000

39. Schober M, Raghavan S, Nikolova M, Polak L, Pasolli HA, Beggs HE, Reichardt LF, Fuchs E: Focal adhesion kinase modulates tension signaling to control actin and focal adhesion dynamics. *J Cell Biol* 176: 667–680, 2007
40. Asanuma K, Yanagida-Asanuma E, Faul C, Tomino Y, Kim K, Mundel P: Synaptopodin orchestrates actin organization and cell motility *via* regulation of RhoA signalling. *Nat Cell Biol* 8: 485–491, 2006
41. de Jong PE, Brenner BM: From secondary to primary prevention of progressive renal disease: The case for screening for albuminuria. *Kidney Int* 66: 2109–2118, 2004
42. Bains R, Furness PN, Critchley DR: A quantitative immunofluorescence study of glomerular cell adhesion proteins in proteinuric states. *J Pathol* 183: 272–280, 1997
43. Takagi C, Ueki K, Ikeuchi H, Kuroiwa T, Kaneko Y, Tsukada Y, Maezawa A, Mitaka T, Sasaki T, Nojima Y: Increased expression of cell adhesion kinase beta in human and rat crescentic glomerulonephritis. *Am J Kidney Dis* 39: 174–182, 2002
44. Morino N, Matsumoto T, Ueki K, Mimura T, Hamasaki K, Kanda H, Naruse T, Yazaki Y, Nojima Y: Glomerular overexpression and increased tyrosine phosphorylation of focal adhesion kinase p125FAK in lupus-prone MRL/MP-lpr/lpr mice. *Immunology* 97: 634–640, 1999
45. Tang H, Kerins DM, Hao Q, Inagami T, Vaughan DE: The urokinase-type plasminogen activator receptor mediates tyrosine phosphorylation of focal adhesion proteins and activation of mitogen-activated protein kinase in cultured endothelial cells. *J Biol Chem* 273: 18268–18272, 1998
46. Aguirre Ghiso JA: Inhibition of FAK signaling activated by urokinase receptor induces dormancy in human carcinoma cells in vivo. *Oncogene* 21: 2513–2524, 2002
47. Hsia DA, Mitra SK, Hauck CR, Streblow DN, Nelson JA, Ilic D, Huang S, Li E, Nemerow GR, Leng J, Spencer KS, Cheresh DA, Schlaepfer DD: Differential regulation of cell motility and invasion by FAK. *J Cell Biol* 160: 753–767, 2003
48. del Pozo MA, Price LS, Alderson NB, Ren XD, Schwartz MA: Adhesion to the extracellular matrix regulates the coupling of the small GTPase Rac to its effector PAK. *EMBO J* 19: 2008–2014, 2000
49. Polte TR, Hanks SK: Interaction between focal adhesion kinase and Crk-associated tyrosine kinase substrate p130Cas. *Proc Natl Acad Sci U S A* 92: 10678–10682, 1995
50. Visse R, Nagase H: Matrix metalloproteinases and tissue inhibitors of metalloproteinases: Structure, function, and biochemistry. *Circ Res* 92: 827–839, 2003
51. Shankland SJ, Pippin JW, Reiser J, Mundel P: Podocytes in culture: Past, present, and future. *Kidney Int* 72: 26–36, 2007
52. Takemoto M, Asker N, Gerhardt H, Lundkvist A, Johansson BR, Saito Y, Betsholtz C: A new method for large scale isolation of kidney glomeruli from mice. *Am J Pathol* 161: 799–805, 2002
53. Ishibe S, Karihaloo A, Ma H, Zhang J, Marlier A, Mitobe M, Togawa A, Schmitt R, Czyczk J, Kashgarian M, Geller DS, Thorgeirsson SS, Cantley LG: Met and the epidermal growth factor receptor act cooperatively to regulate final nephron number and maintain collecting duct morphology. *Development* 136: 337–345, 2009
54. Katsuya K, Yaoita E, Yoshida Y, Yamamoto Y, Yamamoto T: An improved method for primary culture of rat podocytes. *Kidney Int* 69: 2101–2106, 2006
55. Ishibe S, Haydu JE, Togawa A, Marlier A, Cantley LG: Cell confluency regulates Hgf-stimulated cell morphogenesis in a beta-catenin dependent manner. *Mol Cell Biol* 26: 9232–9243, 2006
56. Ishibe S, Joly D, Zhu X, Cantley LG: Phosphorylation-dependent paxillin-ERK association mediates hepatocyte growth factor-stimulated epithelial morphogenesis. *Mol Cell* 12: 1275–1285, 2003
57. Brinkkoetter PT, Olivier P, Wu JS, Henderson S, Krofft RD, Pippin JW, Hockenbery D, Roberts JM, Shankland SJ: Cyclin I activates Cdk5 and regulates expression of Bcl-2 and Bcl-XL in postmitotic mouse cells. *J Clin Invest* September 1, 2009 [epub ahead of print]

Supplemental information for this article is available online at http://www.jasn.org/.